

Supplementary Information for

Entropic contributions to the stability of electrochemically adsorbed anion layers on Au(111), a microcalorimetric study

Marco Schönig and Rolf Schuster

Institute of Physical Chemistry, Karlsruhe Institute of Technology, Kaiserstraße 12, 76131 Karlsruhe, Germany

1. Experimental Details

As pointed out in the main text the electrochemical and calorimetric measurements were conducted in a home-built calorimeter, which was previously introduced in ref. ¹ and ². In this setup, a thin working electrode (WE) was directly placed on top of a 25 μm thick LiTaO_3 pyroelectric sensor. The WE for all measurements in this contribution was a 200 nm Au film evaporated onto a 50 μm thick optically polished, c-cut sapphire sheet (Kyburz) in a home-built evaporation chamber. Between the WE and the sensor an additional 50 μm sapphire sheet was placed to avoid influences of electrostriction. The usage of a thin working electrode together with mechanical compression of the whole assembly ensured good heat conduction between electrode and sensor. The electrochemical cell, which was made of Kel-F, was placed on top of the WE and was sealed with an O-Ring (Viton) against leakage. For each experimental assembly a new Au-film electrode, which was stored in a tube oven at 600°C after the evaporation process, was flame annealed in a butane-gas flame and mounted in the calorimeter under Ar atmosphere. Thermal evaporation of gold on c-cut sapphire was shown to yield preferentially (111)-terminated gold domains. ³ Flame annealing removes contaminants and substantially increases the grain size. ⁴ Directly after assembly the cell was filled with the electrolyte solution, which was deaerated by Ar bubbling. The solutions were prepared from ultrapure water (18.2 Ωcm , Arim, Sartorius) and KCl (Alfa Aesar, Puratronic), KBr (Alfa Aesar, Puratronic), KI (Alfa Aesar, 99.9% metals basis), LiCl (Merck, pro analysi), CsCl (Merck, suprapur) and H_2SO_4 (Merck, suprapur). Pt wires served as counter and pseudo-reference electrode. To achieve a better comparability with the literature we referenced the potential given in the paper to the SCE scale by adjusting the potential of the first sharp peak of the respective CV of each anion to the corresponding potential of this peak obtained by Lipkowski et al. using Au(111) single-crystal electrodes with a SCE reference electrode. ⁵

2. Determination of the reaction entropy from microcalorimetric measurements

For Fig.1 of the main text, the reaction entropy was obtained by two different experimental procedures, namely, by the application of continuous current pulses with constant amplitude, starting under open circuit conditions, and by a series of potential pulses with varying amplitudes, starting from a fixed rest potential. For more details c. f. supporting information of ref ⁶.

Continuous current pulses starting from open circuit conditions:

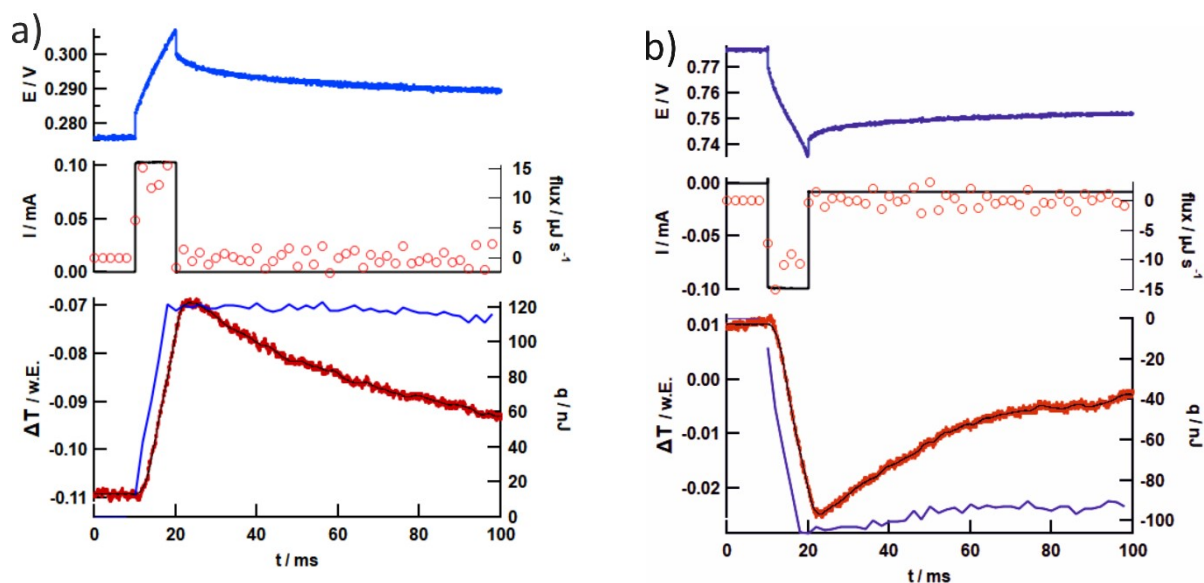


Figure S1: Potential E (blue, left axis), current I (black, left axis) and temperature ΔT (red line, left axis) transients, resulting from a) a 10 ms, +100 μA current pulse starting at 0.27 V and b) a 10 ms, -100 μA current pulse starting at 0.78 V for Au(111) in 0.1 M KCl. In addition the heat flux (red circles, right axis), obtained by deconvolution of the temperature transients is given in the middle panel and the absolute exchanged heat (blue, right axis) is given in the lower panel.

The first method uses 10 ms current pulses with a constant amplitude in order to sweep through a potential region continuously. Representative potential-, current- and temperature transients for this method at two different potentials in the adsorption region of Cl^- are shown in Figs. S1a and S1b. At $t = 10$ ms, a 100 μA positive/negative current pulse is applied (black, middle panel), starting from open circuit conditions, resulting in a linear potential increase (blue, upper panel) due to (pseudo-) capacitive double-layer charging. At $t = 20$ ms the cell is switched back to open circuit conditions, which is accompanied by a small potential relaxation. Note that the steep vertical potential changes are caused by the IR-drop due to the electrolyte resistance. The cell is held under open circuit conditions for 1 s, after which a consecutive pulse with the same current amplitude is applied, now starting from a slightly higher rest potential.

Upon application of a positive current pulse, the temperature (red, lower panel) instantly rises and relaxes back to the initial value after switching to open circuit conditions. The maximum temperature change is reached slightly after $t = 20$ ms. Using the temperature response function of our cell, measured with 2 ms laser pulses, we reconstructed the heat flux caused by the current pulse (red dots, middle panel) according to ref ⁷. By integration of the heat flux, we obtained the total heat (blue, lower panel) as a function of time. The total heat increases linearly during the current pulse and stays constant after the current is switched off. This signals that the anion adsorption process is essentially completed during the 10 ms pulse. To calculate the reaction entropy, we thus used the total heat directly after the pulse at $t = 20$ ms. By dividing the total heat by the charge, which flowed during the current pulse, we obtain the heat per mole of elementary charges which is the molar heat of the adsorption process. Positive molar heat means warming of the electrode upon the anodic process. Using continuous current pulses irreversible contributions to the heat, due to the deviation from equilibrium during the current flow, are included in the measured heat. Nevertheless, since we

are using small current amplitudes, the resulting overpotential is small and thereby the irreversible heat contribution is also small. Indeed, in Fig.1 of the main text the difference between entropies calculated from positive and negative current pulses is very small (typically well below $10 \text{ J mol}^{-1} \text{ K}^{-1}$) and therefore the molar heat is close to the reversibly exchanged molar heat, i.e., the Peltier heat Π .

The Peltier heat is the sum of the entropy change resulting from the electrochemical half-cell reaction $\Delta_R S$ and the entropy changes resulting from charge transport across the boundaries of the half-cell $\Delta_T S$ (for a theoretical derivation c. f. ref ⁸)

$$\Pi = -T(\Delta_R S + \Delta_T S) \quad (S1).$$

Following the procedure described in the supplement of ref. ⁹, the entropy change due to transport can be calculated from the Eastman entropies of transport \hat{s}_i of the ions i and their Hittorf transference numbers t_i ,

$$\Delta_T S = \sum_i \frac{t_i \hat{s}_i}{z_i} \quad (S2).$$

The Eastman entropies of transport used for the calculations are listed in Table S1 and were taken from ref. ⁸. The entropy of transport for electrons is small and is therefore neglected in the above-stated formula¹⁰.

The Hittorf transference numbers were calculated from the limiting ionic conductivities taken from ref. ¹¹ and are also listed in Table S1. The last column of the table also contains the resulting transport entropy changes $\Delta_T S$ calculated with eq. S2.

Potential pulses starting from a constant rest potential:

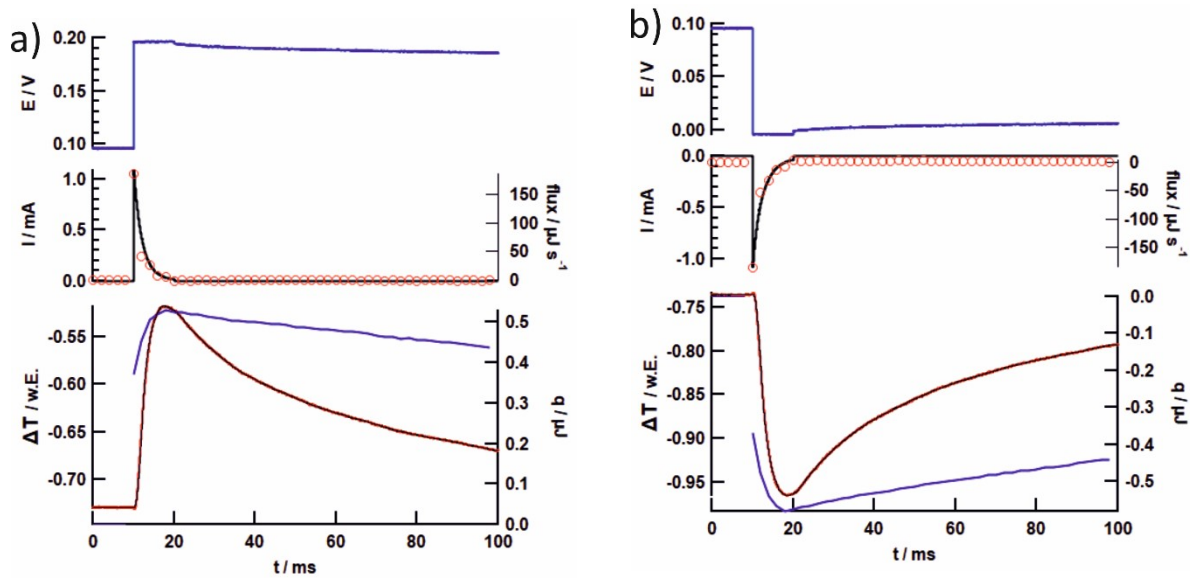


Figure S2: Potential E (blue, left axis), current I (black, left axis) and temperature ΔT (red line, left axis) transients, resulting from a) a 10 ms, +100 mV current pulse and b) a 10 ms, -100 mV current pulse, starting at 0.1 V for Au(111) in 0.1 M KCl. In addition, the heat flux (red circles, right axis), obtained by deconvolution of the temperature transients is given in the middle panel and the absolute exchanged heat (blue, right axis) is given in the lower panel.

Transients for the second experimental procedure, using potential pulses starting from a constant rest potential, are shown in Figs. S2a and S2b. Upon application of a 10 ms potential pulse the current rises sharply and afterwards decays ‘exponentially’. Similar to the behaviour seen in Figs. S1a and S1b, the heat flux directly follows the current flow. As for the continuous current pulses we used the total heat at $t = 20$ ms to derive the molar heat. Since we applied different overpotentials at the same rest potential, we are able to eliminate the irreversible heat contribution by extrapolating the molar heat obtained with different overpotentials to zero overpotential (c.f. ref ⁷). From the reversibly exchanged molar heat, the reaction entropy was calculated in the same way as pointed out above for continuous current pulses. As visible in Fig.1 of the main text, the reaction entropy obtained by potential pulses falls within the values obtained by positive and negative continuous current pulses. This shows that the exchanged heat upon anion adsorption/desorption is indeed very reversible and the error stemming from statistical fluctuations and irreversible heat is typically within ± 7 J mol⁻¹ K⁻¹.

Table S1: Hittorf transference numbers t_i and Eastman entropies of transport \hat{s}_i taken from ref.⁸ and the resulting transport entropies $\Delta_T S$. ^a The Eastman entropy of transport of bisulfate ions is assumed to be -3 J mol⁻¹ K⁻¹ in accordance with ref ¹².

t_i	H ⁺	Li ⁺	K ⁺	Cs ⁺	I ⁻	Br ⁻	Cl ⁻	SO ₄ ²⁻	HSO ₄ ⁻	$\Delta_T S /$ J mol ⁻¹ K ⁻¹
0.1 M H ₂ SO ₄	0.851	-	-	-	-	-	-	0.073	0.076	35.8
0.1 M KI	-	-	0.491	-	0.509	-	-	-	-	-7.0
0.1 M KBr	-	-	0.487	-	-	0.513	-	-	-	-3.1
0.1 M LiCl	-	0.337	-	-	-	-	0.663	-	-	1.0
0.1 M KCl	-	-	0.492	-	-	-	0.508	-	-	-3.3
0.1 M CsCl	-	-	-	0.503	-	-	0.497	-	-	-6.3
$\hat{s} /$ J mol ⁻¹ K ⁻¹	43	-3	7	13	-7	0	0	27	-3 ^a	-

2. Determination of the reaction entropy as function of the anion coverage

Figure 2 in the main text shows the reaction entropy for chloride adsorption from 0.1 M KCl on Au(111) as a function of the anion coverage. To determine the anion coverage we extracted the surface excess concentration from the results of chronocoulometric measurements by the group of Lipkowski as a function of potential (ref. ⁵, Fig. 1) using the software Engauge Digitizer. ¹³ The so received data was up-sampled by a factor of 100, using an interpolation low-pass-filter of 3 data points. We thereby could allocate the respective surface excess concentration, to each potential value. The anion coverage is then given by division of the surface excess concentration at each potential by the maximum halide surface concentration taken from ref. ⁵. Since the rest potentials of the continuous current pulse series slightly vary between each series, we binned the data shown in Fig.1 of the main text for each anion before allocating. For that purpose, we divided a potential interval of 1 V, centred at the reaction entropy minimum, into 50 bins with a width of 20 mV and sorted the reaction entropy values for each series in the respective bins. The bin size was chosen, so that each bin in the adsorption region was filled with at least two data values. The reaction entropies as a function of anion coverage of the other anions introduced in Fig. 1 of the main text are shown in Fig S3.

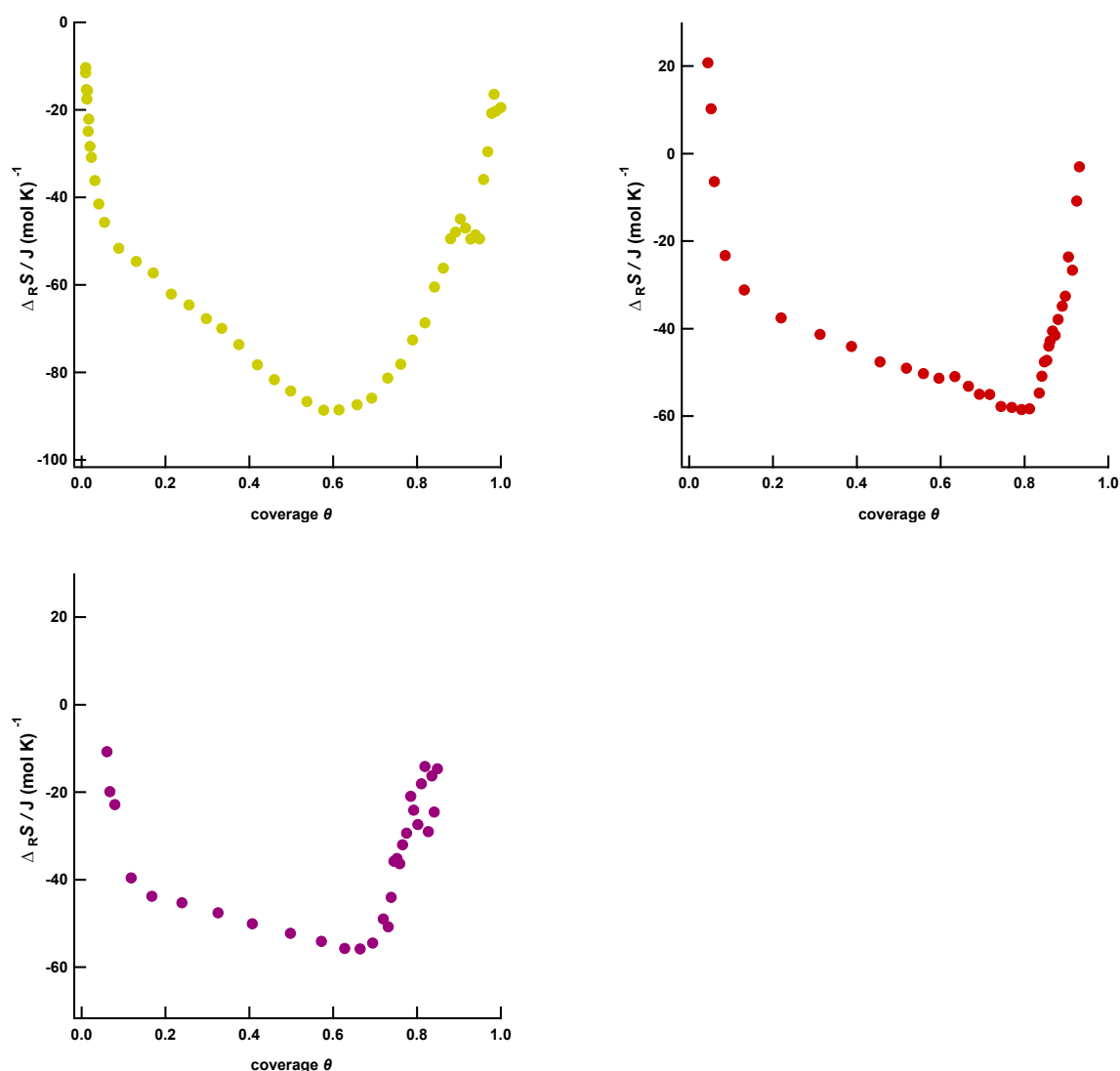


Figure S3: Averaged reaction entropy data from Fig.1 as function of the anion coverage of the respective anion: a) bromide (red), b) iodide (purple) and sulfate (yellow).

3. Quasi-chemical approximation

Molar entropy of a lattice-gas according to the quasi-chemical approximation

To describe the entropy of arrangements of particles on a surface in the presence of interactions the ideal lattice-gas, i.e., the Langmuir model presented in the main text (eq. 2) is not sufficient. This holds true for mean-field approximations, like, e.g., the Bragg-Williamson approximation, since also in these models all surface sites are occupied with the same probability. Deviations from the ideal lattice-gas entropy can be accounted for by using the quasi-chemical approximation in which pair-interactions between nearest neighbours are considered, resulting in a statistical distribution of contact pairs on the surface. A representation of the chemical potential of the particles within this model was for example given by Koper: ¹⁴

$$\mu_{qc} = -RT \ln \left[\frac{\theta}{1-\theta} \left(\frac{(1-\theta)\{A-1+2\theta\}}{\theta\{A+1-2\theta\}} \right)^{c/2} \right], \quad (S3)$$

with A as:

$$A = 1 - 4(1-\theta)\theta \left(1 - e^{-\frac{w(\theta)}{kT}} \right), \quad (S3.1)$$

where $w(\theta)$ describes the pair-interaction energy and which itself can be a function of coverage. c is the coordination number, which in the case of the hexagonal lattice is 6 and the other symbols have their usual meaning. For obtaining the partial molar configurational entropy of this lattice-gas, we differentiated the chemical potential μ_{qc} (eq. S3) with respect to the temperature T . The differentiation resulted in the partial molar configurational entropy:

$$s_{QCA} = \frac{R\theta^2 T (B-C)(\sqrt{A}-2\theta+1)^3}{(1-\theta)^2 (\sqrt{A}+2\theta-1)^3} - R \ln \left(\frac{(1-\theta)^2 (\sqrt{A}+2\theta-1)^3}{\theta^2 (\sqrt{A}-2\theta+1)^3} \right), \quad (S4)$$

with:

$$B = \frac{6(1-\theta)^3 w(\theta) e^{-\frac{w(\theta)}{kT}} (\sqrt{A}+2\theta-1)^2}{k\theta T^2 \sqrt{A} (\sqrt{A}-2\theta+1)^3}, \quad (S4.1)$$

and

$$C = \frac{6(1-\theta)^3 w(\theta) e^{-\frac{w(\theta)}{kT}} (\sqrt{A}+2\theta-1)^3}{k\theta T^2 \sqrt{A} (\sqrt{A}-2\theta+1)^4}. \quad (S4.2)$$

Molar entropy in the presence of repulsive Coulomb-interactions

In the main text we assumed dipole-dipole interactions between the adsorbed anion/substrate dipoles, represented by $w(\theta)$ given by eq. 3 in the main text. Here, for illustration purposes we consider repulsive Coulomb-interactions between the adsorbed halide ions, ignoring the counter charge in the substrate. The pair interaction energy would then arise from Coulombic charge repulsion: ¹⁵

$$w(\theta) = \frac{q^2}{\epsilon_0 \cdot R} \theta^{1/2}, \quad (S5)$$

where q is the charge of the adsorbed species, ϵ_0 is the vacuum permittivity and R is the nearest-neighbour distance. In this picture, the ions will be partially discharged by a fraction y upon adsorption, which is included by using $q = (1 - y)e$ for the monovalent halide ions. Since it is commonly believed that the halide anions are to a large extent discharged,¹⁶ we included the partial molar entropy resulting from the QCA for several y values ranging from 0.9 (100 kJ mol⁻¹, black), 0.95 (20 kJ mol⁻¹, wine), 0.97 (10 kJ mol⁻¹, red), and 0.98 (5 kJ mol⁻¹, orange) in Fig. S3 together with the averaged experimental reaction entropy in 0.1 M KCl on Au(111) from Figs. 2 or 3 of the main text. It is readily visible from Fig. S3 that no y parameter can reasonably describe the measured reaction entropy.

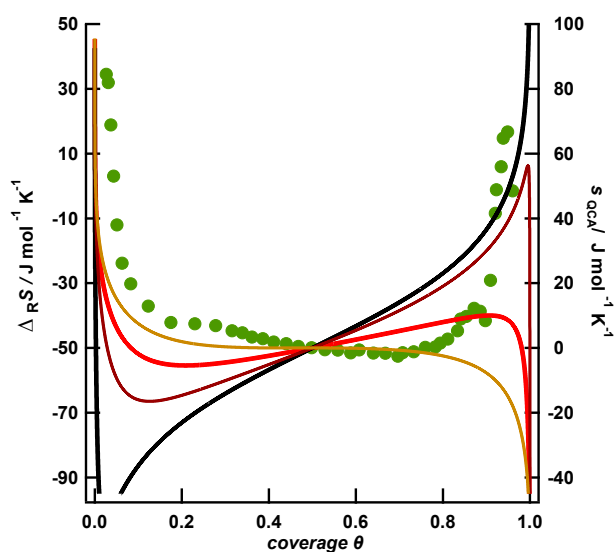


Figure S4: Comparison of the experimental reaction entropy for the adsorption of Cl⁻ on Au(111) with the configurational entropy of a lattice-gas with repulsive Coulomb interactions, described within the quasi-chemical approximation according to eq. S5. The different repulsive interaction energies w at full coverage were: 100 kJ mol⁻¹ (black), 20 kJ mol⁻¹ (wine), 10 kJ mol⁻¹ (red) and 5 kJ mol⁻¹ (orange), corresponding to partial discharging of $y = 0.9, 0.95, 0.97,$ and 0.98 .

References

- 1 K. D. Etzel, K. R. Bickel and R. Schuster, *Rev. Sci. Instr.*, 2010, **81**, 34101.
- 2 S. Frittmann, V. Halka, C. Jaramillo and R. Schuster, *Rev. Sci. Instr.*, 2015, **86**, 64102.
- 3 a) Y. Ito, K. Kushida and H. Takeuchi, *J. Cryst. Growth*, 1991, **112**, 427; b) G. Kästle, H.-G. Boyen, B. Koslowski, A. Plettl, F. Weigl and P. Ziemann, *Surf. Sci.*, 2002, **498**, 168;
- 4 M. H. Dishner, M. M. Ivey, S. Gorer, J. C. Hemminger and F. J. Feher, *J. Vac. Sci. Technol*, 1998, **16**, 3295.
- 5 J. Lipkowski, Z. Shi, A. Chen, B. Pettinger and C. Bilger, *Electrochim. Acta*, 1998, **43**, 2875.
- 6 S. Frittmann, V. Halka and R. Schuster, *Angew. Chem.*, 2016, **55**, 4688.
- 7 K. R. Bickel, K. D. Etzel, V. Halka and R. Schuster, *Electrochim. Acta*, 2013, **112**, 801.
- 8 J. N. Agar, in *Advances in Electrochemistry and Electrochemical Engineering*, vol. 3, pp. 31–121.
- 9 M. Schönig, S. Frittmann and R. Schuster, *ChemPhysChem*, 2022.
- 10 a) T. Ozeki, N. Ogawa, K. Aikawa, I. Watanabe and S. Ikeda, *J. Electroanal. Chem.*, 1983, **145**, 53; b) A. L. Rockwood, *Thermochim. Acta*, 2009, **490**, 82;
- 11 Lide D. R., ed., *CRC handbook of chemistry and physics. A ready-reference book of chemical and physical data*, CRC Press, Boston, 71st edn., 1990.
- 12 S. Frittmann and R. Schuster, *J. Phys. Chem. C*, 2016, **120**, 21522.
- 13 Mark Mitchell, Baurzhan Muftakhidinov and Tobias Winchen, "Engauge Digitizer Software (12.1)" <http://markummittchell.github.io/engauge-digitizer>, Last Accessed: 26. September 2022.
- 14 M. T. M. Koper, *J. Electroanal. Chem.*, 1998, **450**, 189.
- 15 B. E. Conway and H. Angerstein-Kozłowska, *J. Electroanal. Chem.*, 1980, **113**, 63.
- 16 O. M. Magnussen, *Chem. Rev.*, 2002, **102**, 679.